Journal of the Optical Society of America B
OPTICAL PHYSICS

Effect of atomic diffusion on the Raman–Ramsey coherent population trapping resonances

ELENA KUCHINA,[1] EUGENIY E. MIKHAILOV,[2] AND IRINA NOVIKOVA[2,*]

[1]Thomas Nelson Community College, Hampton, Virginia 23666, USA
[2]Department of Physics, College of William and Mary, Williamsburg, Virginia 23188, USA
*Corresponding author: ixnovi@wm.edu

Received 24 November 2015; revised 12 January 2016; accepted 2 February 2016; posted 5 February 2016 (Doc. ID 254508); published 11 March 2016

We experimentally investigated the characteristics of two-photon transmission resonances in Rb vapor cells with different amounts of buffer gas under the conditions of steady-state coherent population trapping (CPT) and a pulsed Raman–Ramsey (RR) CPT interrogation scheme. We particularly focused on the influence of the Rb atoms diffusing in and out of the laser beam. We showed that this effect modifies the shape of both CPT and RR resonances as well as their projected performance for CPT clock applications. In particular we found that at moderate buffer gas pressures RR-CPT did not improve the projected atomic clock stability compared to the regular steady-state CPT resonance. © 2016 Optical Society of America

OCIS codes: (270.1670) Coherent optical effects; (020.1670) Coherent optical effects; (020.2070) Effects of collisions.

http://dx.doi.org/10.1364/JOSAB.33.000610

1. INTRODUCTION

Precise measurements of energy-level splitting in atoms and molecules are at the heart of many devices. Long-lived transitions between the ground-state hyperfine sublevels of alkali atoms are particularly attractive for practical purposes due to their high quality factor. Because their transition frequencies are typically within a few GHz range, there has been a lot of interest in investigating all-optical interrogation methods for development of compact frequency standards and magnetometers [1].

Coherent population trapping (CPT) [2–4] is a two-photon optical effect in which two optical fields form a resonant Λ system based on the two ground hyperfine states, as shown in Fig. 1. Under the two-photon resonance conditions $\omega_{bc} = \nu_1 - \nu_2$, that is, when the difference of the two optical field frequencies $\nu_{1,2}$ matches the energy splitting of the two ground states ω_{bc}, the combined action of the two optical fields optically pumps the atoms into a noninteracting coherent superposition of these two states known as a "dark state" $|D\rangle$:

$$|D\rangle = \mathcal{N}(\Omega_1|c\rangle - \Omega_2|b\rangle), \tag{1}$$

where $\Omega_{1,2}$ are the Rabi frequencies of the two applied optical fields, and $\mathcal{N} = 1/\sqrt{\Omega_1^2 + \Omega_2^2}$ is the normalization constant. Under the CPT conditions the absorption of the atomic medium is suppressed, and one observes a narrow transmission resonance with width γ_{CPT}:

$$\gamma_{\mathrm{CPT}} = \gamma_0 + |\Omega|^2/\Gamma, \tag{2}$$

where the first term represents the dark state decoherence rate γ_0, and the second term demonstrates the CPT resonance power broadening, as $|\Omega|^2 = |\Omega_1|^2 + |\Omega_2|^2$, and Γ is an effective excited state decay rate [5]. In a dilute alkali metal vapor the decoherence rates of the ground-state sublevels are often governed by the thermal motion of the atoms, leading to a relatively long dark state lifetime [6] of a few hundred microseconds for a vapor cell with a buffer gas [7,8] and up to hundreds of milliseconds for the cell with an antirelaxation wall coating [9–12].

In the last few decades CPT resonances have been successfully implemented for both compact and chip-scale atomic clocks and magnetometers [3,4,13,14]. A traditional scheme for a CPT-based frequency standard operation [3] includes a phase-modulated laser (typically a VCSEL) that produces necessary optical fields interacting with atoms in a desired Λ configuration. Adjusting the phase modulation frequency precisely to the frequency difference between the two atomic ground levels—the optical transmission peaks—allows the frequency of the laser modulation source to be locked to the atomic frequency. For atomic clocks the external source is typically locked to the magnetic-field insensitive atomic transition, whereas for CPT-based magnetometers the frequency difference between two magnetic-sensitive transitions is measured to extract information about magnetic field value.

There is an ongoing effort to improve the characteristics of CPT resonances; for example, to reduce their sensitivity to various technical noises (laser intensity and frequency noise, fluctuations of environmental conditions) or to increase their

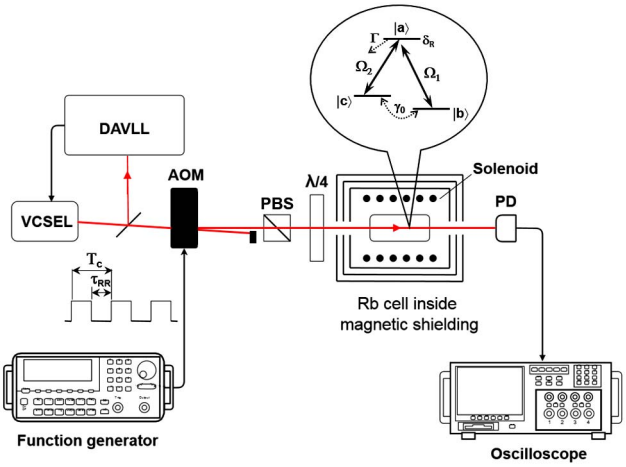

Fig. 1. Schematic of the experimental setup. The power and polarization of the optical field before the Rb vapor cell is controlled using an AOM, a polarizing beam splitter (PBS), and a quarter wave plate ($\lambda/4$). To stabilize the frequency of the VCSEL, approximately 20% of its output is reflected into the DAVLL block, consisting of an auxiliary vapor cell in strong magnetic field, a quarter wave plate, and a balanced PD [28]. Inset shows the simplified level structure of Rb atoms.

contrast. It has been demonstrated that tracking the time evolution of the dark state (similar to the more traditional Ramsey scheme with two separated interrogation zones [15]) offers several important advantages over traditional steady-state CPT transmission measurements. This so-called Raman–Ramsey (RR) interaction [16] works as follows: first, the bichromatic optical field is turned on for long enough to prepare atoms in the dark state; then, the optical field is turned off for the time τ_{RR}, and the dark state is allowed to freely evolve in the dark; finally, the optical field is turned on again, and its transmission after the time τ_m is monitored. In case of nonzero two-photon detuning, the dark state is not stationary, but it acquires an extra relative phase during its time evolution:

$$|D(\delta_R)\rangle = \mathcal{N}(\Omega_1|c\rangle - \Omega_2 e^{i\delta_R\cdot\tau_{RR}}|b\rangle), \tag{3}$$

where $\delta_R = \omega_{bc} - \nu_1 + \nu_2$ is the two-photon Raman detuning. It is easy to see now that after the time $\tau_{RR} = \pi/\delta_R$ the original dark state evolves into the strongly interacting bright state, and if the relative phases of the two optical fields are maintained, instead of enhanced transmission, one observes enhanced absorption. It is also clear that the oscillations between extra transmission and absorption should be a periodic function of the evolution time τ_{RR}, as long as this time is shorter than the ground-state coherence lifetime. Assuming the homogeneity of the ground-state decoherence (i.e., that all atoms experience the same ground-state decay rate γ_0), it is possible to calculate the expected RR-CPT absorption coefficient κ_{RR} [17]:

$$\kappa_{RR} = \alpha(1 + \beta e^{-\gamma_0\tau_{RR}}\cos(\delta_R\tau_{RR} - \Phi)), \tag{4}$$

where the values of the coefficients α, β, and Φ are calculated in Ref. [17].

Several publications theoretically and experimentally demonstrated the advantages of the RR interrogation method compared to the traditional cw CPT [18–22]. In addition to typically having a larger contrast, an attractive feature of RR-CPT resonance is that the width of the observed resonances is determined only by the evolution time and does not depend on laser power, unlike the regular CPT resonance. Thus, such resonances are not susceptible to power broadening and light shifts, as was demonstrated in several publications [19,22,23]. In particular, one can show that for a homogeneously power-broadened CPT resonance, in which all atoms have the same ground-state decoherence rate, the expected enhancement in the signal-to-noise ratio is

$$\frac{\mathrm{SNR}_{RR}}{\mathrm{SNR}_{CPT}} = 2(\pi\tau_{RR}\gamma_0)^2\frac{C_{RR}}{C_{CPT}}\sqrt{\frac{\tau_m I_{RR}}{T_c I_{CPT}}}, \tag{5}$$

where T_c is the total duration of one Ramsey pulse sequence, I_{RR} and I_{CPT} are the corresponding average background intensities (i.e., light intensities away from CPT conditions), $C_{CPT} = I(\delta_R = 0)/I_{CPT} - 1$ is the contrast of the CPT resonance, and $C_{RR} = \Delta I_{\mathrm{fringe}}/I_{RR}$ is the RR-CPT contrast, where $\Delta I_{\mathrm{fringe}}$ is the amplitude of the central fringe near $\delta_R = 0$ and depends on the specific values of τ_{RR}, τ_m, and so forth. We assume that the ratio of signals in two interrogation schemes is proportional to the ratio of the second derivatives of the light transmission dependences on two-photon detuning. In our calculations, we assumed a Lorentzian line shape of the cw CPT resonance with the minimum width of γ_0 [see Eq. (2)] and the RR-CPT line shape described by Eq. (4). Thus, the product $(\tau_{RR}\gamma_0)^2$ reflects the ratio of these derivatives, and it is easy to estimate that the RR-CPT arrangement is the most advantageous for $\tau_{RR} \sim 1/\gamma_0$. The term under the square root represents the ratio of the shot noise contributions, under the assumption of the shot-noise-limited performance, corrected for the acquisition duty cycle. While the CPT signal is continuous, the RR-CPT signal is collected only for the τ_m/T_c fraction of the time.

In this paper, we consider the case of "inhomogeneously" broadened ground-state coherence, in which different atoms can have substantially different decoherence rates γ_0. This situation often occurs in atomic vapor cells with buffer gas, in which the size of the laser beam is smaller than the vapor cell cross section. In this case, atoms can diffuse out of the interaction volume and then come back after spending some time outside of the laser beams without dephasing their ground-state coherence. Such a diffusion process introduces atoms with a wide range of dark state evolution times inside the interaction region, causing strong modifications in the CPT line shape; in particular, the appearance of a sharp "pointy" top [24,25]. It was shown that such behavior can be qualitatively described similarly to the RR resonances [6,25,26] but by averaging over the possible values of the evolution in the dark time, determined by dynamics of the atomic diffusion.

Below, we experimentally study this different regime for the RR-CPT effect, in which an atom undergoes both controlled and random evolution in the dark, one due to turning the light fields on and off and the other due to the atom temporarily leaving the interaction region. We compare the spectral line shapes of regular CPT resonances (continuous laser interrogation) and RR-CPT resonances (pulsed interrogation) in two different Rb vapor cells with different amounts of buffer gas

(5 and 30 Torr of Ne) and observe a significant modification of the RR-CPT line shape from Eq. (4). We present a brief comparison of the expected sensitivity for the frequency measurements using steady-state CPT and RR-CPT resonances for the Rb vapor cells with different buffer gas pressure and demonstrate that the diffusion-induced line shape modifications change the relative figure of merit between the two interrogation methods.

2. EXPERIMENTAL ARRANGEMENTS

In our experiment, we used a temperature-stabilized VCSEL operating at the Rb D_1 line ($\lambda = 795$ nm). The laser was current modulated at $\nu_{rf} = 6.8347$ GHz such that the laser carrier frequency and the first modulation sideband were tuned to the $5S_{1/2}F = 2 \rightarrow 5P_{1/2}F' = 1$ and $5S_{1/2}F = 1 \rightarrow 5P_{1/2}F' = 1$ transitions of ^{87}Rb, respectively. The two-photon Raman detuning δ_R was controlled by adjusting the laser microwave modulation frequency ν_{rf} around the value of the ^{87}Rb hyperfine splitting using a computer-controlled homemade microwave source [27], such that $\delta_R = \nu_{rf} - 6.834687135$ GHz. The intensity ratio between the sideband and the carrier was adjusted by changing the modulation power sent to the VCSEL, which kept the sideband to carrier ratio equal to 60%. The optical frequency of the laser was stabilized using a dichroic-atomic-vapor laser lock (DAVLL) [28]. The details of the construction and operation of the homemade laser system are provided in [29].

The circularly polarized laser beam with maximum total power 90 μW and a slightly elliptical Gaussian profile (1.8 and 1.4 mm full width at half-maximum [FWHM]) traversed a cylindrical Pyrex cell (length 75 mm; diameter 22 mm) containing isotopically enriched ^{87}Rb vapor and either 5 or 30 Torr of Ne buffer gas. The cell was mounted inside a three-layer magnetic shielding and actively temperature stabilized at 53°C. To isolate the magnetic field-insensitive CPT resonance, we applied a homogeneous longitudinal magnetic field of 520 mG using a solenoid mounted inside the innermost magnetic shield. Changes in the total laser transmission were recorded using a photodetector (PD), placed after the Rb cell.

For the RR-CPT measurements, we turned the laser beam on and off using an acousto-optical modulator (AOM), placed before the vapor cell, modulated with a square wave at the frequency f_{mod}. We verified that each "on" half-cycle was long enough to achieve the steady-state CPT conditions. The following half-cycle, which corresponded to the AOM "off" period, served as the dark evolution time $\tau_{\mathrm{RR}} = (2f_{\mathrm{mod}})^{-1}$. To reproduce the RR signal, shown in Figs. 2(c)–2(f), the values of the laser transmission were recorded $\tau_m = 20$ μs after the laser was turned on again. This value of τ_m has been chosen to maximize the recorded RR-CPT signal. For longer τ_m the fringe contrast was starting to decrease; for shorter τ_m the overall transmission was smaller even though the line shape was preserved, as we carefully verified.

3. EXPERIMENTAL RESULTS

Figures 2(a) and 2(b) present sample spectra of steady-state CPT resonances recorded in the Rb vapor cells with different amounts of the buffer gas under otherwise identical experimental conditions. For atoms traversing the illuminated interaction

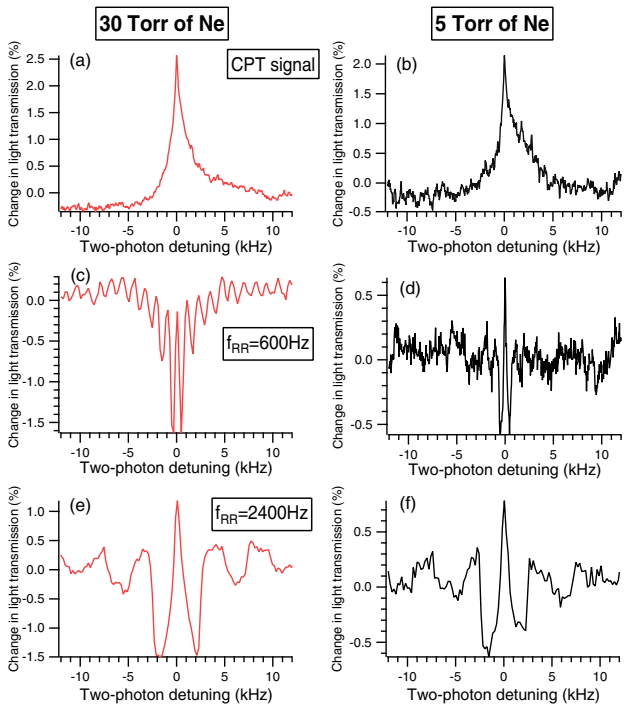

Fig. 2. Examples of steady-state CPT resonances (top row) and RR resonances obtained for different modulation frequencies f_{mod} and, hence, for different dark time intervals (two bottom rows). The left column corresponds to the signals obtained in the Rb cell with 30 Torr of Ne buffer gas, and the right one in the Rb cell with 5 Torr of Ne buffer gas. In all graphs the vertical axis represents the relative optical transmission $I(\delta_R)/I_{\mathrm{background}} - 1$. Two zero points on the 5 Torr graph at $f_{\mathrm{mod}} = 150$ and 300 Hz signify the absence of a detectable signal at such long evolution times.

region only once, the dark state lifetime can be estimated from the average diffusion time through the laser beam of radius a [30], implying the decoherence rate to be

$$\gamma_0 \simeq (2.405)^2 D_0 \frac{p_0}{p} \frac{1}{a^2}, \tag{6}$$

where $D_0 = 0.2$ cm^2/s is the diffusion constant of Rb atoms in Ne at the atmospheric pressure $p_0 = 760$ Torr, and p is the buffer gas pressure inside the cell. Also, because in this case all atoms experience approximately the same ground-state decoherence rate, the CPT line shape is expected to be Lorentzian [this is the necessary assumption for deriving Eq. (5)]. In this model the expected minimum FWHM values for the CPT resonance in the cells with 5 and 30 Torr of Ne buffer gas are 5.6 kHz and 930 Hz, respectively. In our experiments, however, the measured FWHM values for the CPT resonances were quite similar in both cells: ≈1300 Hz and ≈1100 Hz. Also, the shapes of the resonances were clearly non-Lorentzian, indicating the contributions from atoms with a wide range of ground-state decoherence rates.

The pointy line shape analysis of these resonances reveals a strong influence of atomic diffusion in and out of the laser beam [6,24–26]. To understand the origin of the CPT linewidth narrowing, one must take into account the possibility of an atom to leave the interaction region and then return after

some time without dephasing its quantum state. Such a repeated interaction model, developed in Refs. [25,26], draws on parallels between the atom multiple interactions with the laser beams interspersed with the "evolution in the dark" while the atom is outside of the interaction region with the RR-CPT resonances where the time of the evolution in the dark is controlled by turning on and off the laser fields. However, because now the evolution time is governed by the diffusion dynamics and thus stochastic, the resulting signal is effectively averaged over the distribution of the evolution times, which interferes constructively only for $\delta_R = 0$, leading to a "peaky" CPT resonance.

Next, we analyze the effect of such diffusive atomic motion on the RR-CPT resonances. The examples of RR-CPT fringes recorded in both vapor cells at two different AOM modulation frequencies are shown in Figs. 2(c)–2(f). For the $f_{\mathrm{mod}} = 600$ Hz ($\tau_{\mathrm{RR}} = 830$ μs), the recorded transmission signals resemble the traditional RR-CPT fringes, for which the dark evolution time is comparable to the dark state decoherence time: a few higher-contrast fringes near $\delta_R = 0$, and the reduced contrast fringes for larger Raman detunings. Interestingly, the relative heights of the central fringe in the two cells are almost the same, even though one might not have expected to see any fringes for such a long dark time for the cell with 5 Torr of Ne because the diffusion time of Rb atoms through the laser beams is only ≈60 μs. This indicates that the observed RR fringes are mainly due to the atoms that preserved their dark state after leaving the illuminated region and then diffused back after τ_{RR} time. Clearly, the coherence lifetime for such atoms is not limited by the time of flight through the laser beam but rather by their in-and-out diffusion time, which can be significantly longer [25].

In the RR-CPT spectra recorded for the shorter dark evolution time (modulation frequency $f_{\mathrm{mod}} = 2400$ Hz, $\tau_{RR} = 210$ μs) the shape of the fringes changes: there is a clear sharp peak at zero Raman detuning, similar to the sharp peak observed for CPT resonances, with some additional sharp dispersion-like structures for δ_R equal to the multiple of f_{mod}. The shape of the central fringe implies significant contribution from the atoms with diffusion times longer than τ_{RR} because these atoms experience similar distributions of dark evolution times, and their sensitivity to small changes of δ_R is similar for both steady-state CPT or RR-CPT detection schemes.

To verify this statement and to estimate the projected performance of a possible frequency standard, we calculate the maximum slope of the first derivative of the laser transmission $(\partial I/\partial\delta_R)/I|_{\delta_R=0}$, where I is the measured transmitted intensity. Because the background transmission values in the both cells were similar, the value of this slope can be used to estimate the error signal for the feedback loop when locking the microwave modulation source to a CPT or RR-CPT resonance. The values of measured slopes for the two vapor cells are shown in Fig. 3. It is clear that RR-CPT resonances in the 5 Torr vapor cell do not provide any improvement in performance compared to the standard steady-state CPT arrangement, as the measured slope values are independent of the RR modulation frequency f_m. Indeed, in this regime the longest dark state evolution time is provided by the atom physically diffusing out of the laser beam and coming back, which contributes similarly in

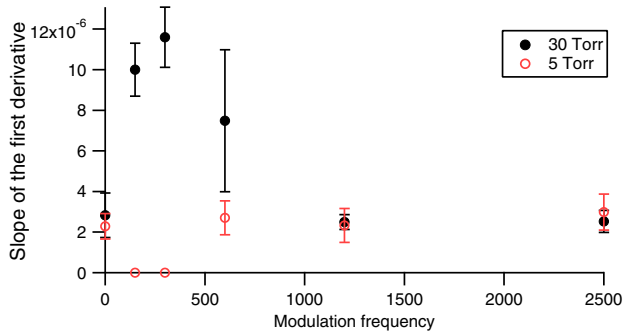

Fig. 3. Estimated value of the error signal slope for atomic clock locking based on the analysis of the measured transmission resonances. Data points corresponding to zero modulation frequency correspond to the steady-state CPT resonances. Each data point is the result of averaging over 5–10 RR-CPT spectra, and error bars represent one standard deviation spread.

the sharpness of the central spectral feature for both CPT and RR-CPT resonances. Thus, having longer or shorter τ_{RR} only affects the number of probed atoms, without changing their response to small changes in the Raman detuning δ_R.

Our measurements in the 30 Torr cell, however, indicated that for lower modulation frequencies there is a clear advantage of using RR-CPT detection method, as we observed an almost sixfold increase of the error signal for $f_m = 300$ Hz. The higher buffer gas pressure slows the diffusion dynamics, and it takes much longer for atoms to leave the interaction region. Still, for shorter dark evolution times τ_{RR} (i.e., for higher modulation frequencies $f_m > 1000$ Hz) the measured maximum slopes of the laser transmission near $\delta_R = 0$ again become comparable to those of the regular CPT resonances, indicating the return to the regime in which the highest spectral sensitivity is determined by the diffusing atoms reentering the laser beam.

4. CONCLUSIONS

We analyzed the RR-CPT spectra, recorded in the Rb vapor cells with 5 and 30 Torr of Ne buffer gas in the regime where the diffusion of the atoms in and out of the illuminated interaction region played a significant role. Previous studies have shown the superiority of the RR-CPT detection compared to the traditional CPT transmission resonances for precise frequency detection in the case of homogeneous ground-state atomic decoherence. In the conditions of our experiments, however, we found that the ratio between the evolution in the dark time of the RR sequence τ_{RR} and the average dark state evolution time of diffusing atoms becomes an important parameter for evaluating the advantages of the RR-CPT method. In particular, we found that in case of shorter τ_{RR} the most sensitive frequency response to the changes of the two-photon Raman detuning is provided by the atoms with long diffusion times, and thus using a more complicated RR-CPT method does not lead to any increase in signal.

Funding. National Science Foundation (NSF) Women in Scientific Education (WISE) (HRD1107147).

Acknowledgment. We acknowledge the support of the National Science Foundation Women in Scientific Education (WISE) Award HRD1107147 for making this collaboration possible. We would like to thank Melissa Guidry for her help at the early steps of the RR setup construction and Owen Wolfe for assistance with the data analysis.

REFERENCES

1. J. Vanier and C. Audoin, *The Quantum Physics of Atomic Frequency Standards* (Adam Hilger, 1989), Vol. **1**.
2. E. Arimondo, "Coherent population trapping in laser spectroscopy," Prog. Opt. **35**, 259–354 (1996).
3. J. Vanier, "Atomic clocks based on coherent population trapping: a review," Appl. Phys. B **81**, 421–442 (2005).
4. V. Shah and J. Kitching, "Advances in coherent population trapping for atomic clocks," in *Advances in Atomic, Molecular, and Optical Physics* (Academic, 2010), Vol. **59**, pp. 21–74.
5. A. Javan, O. Kocharovskaya, H. Lee, and M. O. Scully, "Narrowing of electromagnetically induced transparency resonance in a Doppler-broadened medium," Phys. Rev. A **66**, 013805 (2002).
6. Y. Xiao, "Spectral line narrowing in electromagnetically induced transparency," Mod. Phys. Lett. B **23**, 661–680 (2009).
7. R. Wynands and A. Nagel, "Precision spectroscopy with coherent dark states," Appl. Phys. B **68**, 1–25 (1999).
8. M. Erhard and H. Helm, "Buffer-gas effects on dark resonances: theory and experiment," Phys. Rev. A **63**, 043813 (2001).
9. D. Budker, L. Hollberg, D. F. Kimball, J. Kitching, S. Pustelny, and V. V. Yashchuk, "Microwave transitions and nonlinear magneto-optical rotation in anti-relaxation-coated cells," Phys. Rev. A **71**, 012903 (2005).
10. S. J. Seltzer and M. V. Romalis, "High-temperature alkali vapor cells with antirelaxation surface coatings," J. Appl. Phys. **106**, 114905 (2009).
11. M. V. Balabas, T. Karaulanov, M. P. Ledbetter, and D. Budker, "Polarized alkali-metal vapor with minute-long transverse spin-relaxation time," Phys. Rev. Lett. **105**, 070801 (2010).
12. M. A. Hafiz, V. Maurice, R. Chutani, N. Passilly, C. Gorecki, S. Guérandel, E. de Clercq, and R. Boudot, "Characterization of cs vapor cell coated with octadecyltrichlorosilane using coherent population trapping spectroscopy," J. Appl. Phys. **117**, 184901 (2015).
13. S. Knappe, P. Schwindt, V. Shah, L. Hollberg, J. Kitching, L. Liew, and J. Moreland, "A chip-scale atomic clock based on 87rb with improved frequency stability," Opt. Express **13**, 1249–1253 (2005).
14. S. A. Knappe, "Emerging topics: MEMS atomic clocks," in *Comprehensive Microsystems* (Elsevier, 2008), Vol. **3**, 571–612.
15. J. E. Thomas, P. R. Hemmer, S. Ezekiel, C. C. Leiby, R. H. Picard, and C. R. Willis, "Observation of Ramsey fringes using a stimulated, resonance Raman transition in a sodium atomic beam," Phys. Rev. Lett. **48**, 867–870 (1982).
16. T. Zanon, S. Guerandel, E. de Clercq, D. Holleville, N. Dimarcq, and A. Clairon, "High contrast Ramsey fringes with coherent-population-trapping pulses in a double lambda atomic system," Phys. Rev. Lett. **94**, 193002 (2005).
17. T. Zanon-Willette, E. de Clercq, and E. Arimondo, "Ultrahigh-resolution spectroscopy with atomic or molecular dark resonances: exact steady-state line shapes and asymptotic profiles in the adiabatic pulsed regime," Phys. Rev. A **84**, 062502 (2011).
18. T. Zanon, S. Tremine, S. Guerandel, E. de Clercq, D. Holleville, N. Dimarcq, and A. Clairon, "Observation of Raman–Ramsey fringes with optical CPT pulses," IEEE Trans. Instrum. Meas. **54**, 776–779 (2005).
19. N. Castagna, R. Boudot, S. Guerandel, E. Clercq, N. Dimarcq, and C. Clairon, "Investigations on continuous and pulsed interrogation for a CPT atomic clock," IEEE Trans. Ultrason. Ferroelec. Freq. Contr. **56**, 246–253 (2009).
20. I. Yoshida, N. Hayashi, K. Fujita, S. Taniguchi, Y. Hoshina, and M. Mitsunaga, "Line-shape comparison of electromagnetically induced transparency and Raman–Ramsey fringes in sodium vapor," Phys. Rev. A **87**, 023836 (2013).
21. X. Liu, J.-M. Mérolla, S. Guérandel, E. de Clercq, and R. Boudot, "Ramsey spectroscopy of high-contrast CPT resonances with push-pull optical pumping in Cs vapor," Opt. Express **21**, 12451–12459 (2013).
22. E. Blanshan, S. M. Rochester, E. A. Donley, and J. Kitching, "Light shifts in a pulsed cold-atom coherent-population-trapping clock," Phys. Rev. A **91**, 041401 (2015).
23. G. S. Pati, Z. Warren, N. Yu, and M. S. Shahriar, "Computational studies of light shift in a Raman–Ramsey interference-based atomic clock," J. Opt. Soc. Am. B **32**, 388–394 (2015).
24. I. Novikova, Y. Xiao, D. F. Phillips, and R. L. Walsworth, "EIT and diffusion of atomic coherence," J. Mod. Opt. **52**, 2381–2390 (2005).
25. Y. Xiao, I. Novikova, D. F. Phillips, and R. L. Walsworth, "Diffusion-induced Ramsey narrowing," Phys. Rev. Lett. **96**, 043601 (2006).
26. Y. Xiao, I. Novikova, D. F. Phillips, and R. L. Walsworth, "Repeated interaction model for diffusion-induced Ramsey narrowing," Opt. Express **16**, 14128–14141 (2008).
27. E. E. Mikhailov, T. Horrom, N. Belcher, and I. Novikova, "Performance of a prototype atomic clock based on *lin*∥*lin* coherent population trapping resonances in Rb atomic vapor," J. Opt. Soc. Am. B **27**, 417–422 (2010).
28. V. V. Yashchuk, D. Budker, and J. R. Davis, "Laser frequency stabilization using linear magneto-optics," Rev. Sci. Instrum. **71**, 341 (2000).
29. N. Belcher, E. E. Mikhailov, and I. Novikova, "Atomic clocks and coherent population trapping: experiments for undergraduate laboratories," Am. J. Phys. **77**, 988–998 (2009).
30. W. Happer, "Optical pumping," Rev. Mod. Phys. **44**, 169–249 (1972).